

ROPER ELECTROPRODUCTION AMPLITUDES IN A CHIRAL CONFINEMENT MODEL

M. FIOLHAIS, P. ALBERTO AND J. MARQUES

Departamento de Física and Centro de Física Computacional, Universidade de Coimbra, P-3004-516 Coimbra, Portugal
E-mail: tmanuel@teor.fis.uc.pt

B. GOLLI

Faculty of Education, University of Ljubljana and J. Stefan Institute, Ljubljana, Slovenia

A description of the Roper using the chiral chromodielectric model is presented and the transverse $A_{1/2}$ and the scalar $S_{1/2}$ helicity amplitudes for the electromagnetic Nucleon–Roper transition are obtained for small and moderate Q^2 . The sign of the amplitudes is correct but the model predictions underestimate the data at the photon point. Our results do not indicate a change of sign in any amplitudes up to $Q^2 \sim 1 \text{ GeV}^2$. The contribution of the scalar meson excitations to the Roper electroproduction is taken into account but it turns out to be small in comparison with the quark contribution. However, it is argued that mesonic excitations may play a more prominent role in higher excited states.

1 Introduction

Several properties of the nucleon and its excited states can be successfully explained in the framework of the constituent quark model (CQM), either in its non-relativistic or relativistic version. There are, however, processes where the description in terms of only valence quarks is not adequate suggesting that other degrees of freedom may be important in the description of baryons, in particular the chiral mesons. Typical examples – apart of decay processes – are electromagnetic and weak production amplitudes of the nucleon resonances. Already the production amplitudes for the lowest excited state, the Δ , indicate the important role of the pion cloud in the baryons. The other well known example is the Roper resonance, $N(1440)$, which has been a challenge to any effective model of QCD at low or intermediate energies. Due to the relatively low excitation energy, a simple picture in which one quark populates the $2s$ level does not work. It has been suggested that the inclusion of explicit excitations of gluons and/or glueballs, or explicit excitations of chiral mesons may be necessary to explain its properties.

The other problem related to the CQM is the difficulty to introduce consistently the electromagnetic and the axial currents as well as the interaction

with pions which is necessary to describe the leading decay modes of resonances. Such problems do not exist in relativistic quark models based on effective Lagrangians which incorporate properly the chiral symmetry. Unfortunately, several chiral models for baryons, such as the linear sigma model or various versions of the Nambu–Jona-Lasinio model, though able to describe properly the Δ resonance, are simply not suited to describe higher excited states since they do not confine: for the nucleon, the three valence quarks in the lowest s state are just bound and, for typical parameter sets, the first radial quark excitation already lies in the continuum. In order to resolve this problem, other degrees of freedom have to be introduced in the model to provide binding also at higher excitation energies. The chiral version of the chromodielectric model (CDM) seems to be particularly suitable to describe radial excitations of the nucleon since it contains the chiral mesons as well as a mechanism for confining. The CDM has been used as a model for the nucleon¹ in different approximations. Using the hedgehog coherent state approach supplemented by an angular momentum and isospin projection, several nucleon properties and of the nucleon-delta electromagnetic excitation have been obtained^{1,2,3}.

In the present work we concentrate on the description of the Roper resonance. Its structure and the electroproduction amplitudes have been considered in several versions of the CQM^{4,5,6}. The nature of the Roper resonance has also been considered in a non-chiral version of the CDM using the RPA techniques to describe coupled vibrations of valence quarks and the background chromodielectric field⁷. The energy of the lowest excitation turned out to be 40 % lower than the pure 1s–2s excitations. A similar result was obtained by Guichon⁸, using the MIT bag model and considering the Roper as a collective vibration of valence quarks and the bag.

Our description of baryons in the framework of the CDM model provides relatively simple model states which are straightforwardly used to compute the transverse and scalar helicity amplitudes for the nucleon–Roper transition, in dependence of the photon virtuality⁹. The electromagnetic probe (virtual photon) couples to charged particles, pions and quarks. However, in the CDM, baryons have got a weak pion cloud and therefore the main contribution to the electromagnetic nucleon–Roper amplitudes comes from the quarks.

In Section 2 we introduce the electromagnetic transition amplitudes. In Section 3 we briefly describe the model and construct model states representing baryons, using the angular momentum projection technique from coherent states. In Section 4 we present the CDM predictions for the helicity amplitudes for typical model parameters. Finally, in Section 5 we discuss the contribution of scalar meson vibrations.

2 Electroproduction amplitudes in chiral quark models

In chiral quark models the coupling of quarks to chiral fields is written in the form:

$$\mathcal{L}_{q-\text{meson}} = g \bar{q} (\hat{\sigma} + i \vec{\tau} \cdot \hat{\vec{\pi}} \gamma_5) q . \quad (1)$$

Here g is the coupling parameter related to the mass of the constituent quark $M_q = gf_\pi$. In the CDM the parameter g is substituted by the *chromodielectric* field which takes care of the quark confinement as explained in the next section. In the linear σ -model, in the CDM, as well as in different versions of the Cloudy Bag Model, the chiral meson fields, i.e. the isovector triplet of pion fields, $\vec{\pi}$, and the isoscalar σ field (not present in non-linear versions), are introduced as effective fields with their own dynamics described by the meson part of the Lagrangian:

$$\mathcal{L}_{\text{meson}} = \frac{1}{2} \partial_\mu \hat{\sigma} \partial^\mu \hat{\sigma} + \frac{1}{2} \partial_\mu \hat{\vec{\pi}} \cdot \partial^\mu \hat{\vec{\pi}} - \mathcal{U}(\hat{\sigma}, \hat{\vec{\pi}}) \quad (2)$$

where \mathcal{U} is the Mexican-hat potential describing the meson self-interaction. In different versions of the Nambu–Jona-Lasinio model¹⁰ the chiral fields are explicitly constructed in terms of quark-antiquark excitations of the vacuum in the presence of the valence quarks.

From (2) and from the part of the Lagrangian corresponding to free quarks,

$$\mathcal{L}_q = i \bar{q} \gamma^\mu \partial_\mu q , \quad (3)$$

the electromagnetic current is derived as the conserved Noether current:

$$\hat{J}_{e.m.}^\mu(\mathbf{r}) = \bar{q} \gamma^\mu \left(\frac{1}{6} + \frac{1}{2} \tau_3 \right) q + (\hat{\vec{\pi}} \times \partial^\mu \hat{\vec{\pi}})_3 . \quad (4)$$

Note that the operator contains both the standard quark part as well as the pion part. We stress that in all these models the electromagnetic current operator is derived directly from the Lagrangian, hence no additional assumptions have to be introduced in the calculation of the electromagnetic amplitudes.

We can now readily write down the amplitudes for the electroexcitation of nucleon excited states in terms of the EM current (4). Let us denote by $|\tilde{N}_{M,M_T}\rangle$ and $|\tilde{R}_{J,T;M,M_T}\rangle$ the model states representing the nucleon and the resonant state, respectively (the indexes M and M_T stand for the angular momentum and isospin third components). The resonant transverse and scalar helicity amplitudes, A_λ and $S_{1/2}$ respectively, defined in the rest frame of the resonance, are

$$A_\lambda = -\zeta \sqrt{\frac{2\pi\alpha}{k_W}} \int d^3\mathbf{r} \langle \tilde{R}_{J,T;\lambda,M_T} | \mathbf{J}_{\text{em}}(\mathbf{r}) \cdot \boldsymbol{\epsilon}_{+1} e^{i\mathbf{k}\cdot\mathbf{r}} | \tilde{N}_{\lambda-1,M_T} \rangle \quad (5)$$

$$S_{1/2} = \zeta \sqrt{\frac{2\pi\alpha}{k_W}} \int d\mathbf{r} \langle \tilde{R}_{J,T;+\frac{1}{2},M_T} | J_{\text{em}}^0(\mathbf{r}) e^{i\mathbf{k}\cdot\mathbf{r}} | \tilde{N}_{+\frac{1}{2},M_T} \rangle, \quad (6)$$

where $\alpha = \frac{e^2}{4\pi} = \frac{1}{137}$ is the fine-structure constant, the unit vector ϵ_{+1} is the polarization vector of the electromagnetic field, $k_W = (M_R^2 - M_N^2)/2M_R$ is the photon energy at the photon point (introduced rather than ω which vanishes at $Q^2 = M_R^2 - M_N^2$) and ζ is the sign of the $N\pi$ decay amplitude. This sign has to be explicitly calculated within the model; from (1) in our case. In the case of the Δ resonance ($T = J = \frac{3}{2}$), λ takes two values $\lambda = \frac{3}{2}$ and $\frac{1}{2}$, while for the Roper state ($T = J = \frac{1}{2}$), only one transverse amplitude exists ($\lambda = \frac{1}{2}$).

The photon four momentum is $q^\mu(\omega, \mathbf{k})$ and we define $Q^2 = -q_\mu q^\mu$. In the chosen reference frame the following kinematical relations hold:

$$\omega = \frac{M_R^2 - M_N^2 - Q^2}{2M_R}; \quad \mathbf{k}^2 \equiv k^2 = \left[\frac{M_R^2 + M_N^2 + Q^2}{2M_R} \right]^2 - M_N^2. \quad (7)$$

The electroexcitation amplitudes for the Δ resonance have been analyzed in the framework of chiral quark models^{3,11,12}. They are dominated by the M1 transition but contain also rather sizable quadrupole contributions E2 and C2. The CQM model predicts here too low values for the M1 piece and almost negligible values for the quadrupole amplitudes. In chiral quark models there is a considerable contribution from the pions (i.e. from the second term in (4)): up to 50 % in the M1 amplitude, and they dominate the E2 and C2 pieces. The absolute values of the amplitudes and their behavior as a function of the photon virtuality Q^2 is well reproduced in the linear σ -model. Though the ratios E2/M1 and C2/M1 are also well reproduced in the CDM, this model gives systematically too low values for the amplitudes, which could be attributed to its rather weak pion cloud. As we shall see in Section 4, this might also explain the small values of the Roper production amplitudes at low Q^2 .

In the next section we construct the states $|\tilde{N}\rangle$ and $|\tilde{R}\rangle$ for the Roper in the framework of the CDM and, in Section 4, we present the model predictions for the amplitudes.

3 Baryons in the CDM

The Lagrangian of the CDM contains, apart of the chiral meson fields σ and π , the cromodielectric field χ such that the quark meson-interaction (see (1)) is modified as:

$$\mathcal{L}_{q-\text{meson}} = \frac{g}{\chi} \bar{q} (\hat{\sigma} + i\vec{\tau} \cdot \hat{\vec{\pi}} \gamma_5) q. \quad (8)$$

The idea behind the introduction of the χ field is that it acquires a nonzero expectation value inside the baryon but goes to 0 for larger distances from the center of the baryon, thus pushing the effective constituent quark mass to infinity outside the baryon. In addition, the Lagrangian contains kinetic and potential pieces for the χ -field:

$$\mathcal{L}_\chi = \frac{1}{2} \partial_\mu \hat{\chi} \partial^\mu \hat{\chi} - \frac{1}{2} M_\chi^2 \hat{\chi}^2, \quad (9)$$

where M_χ is the χ mass. In this work we consider only a simple quadratic potential; other versions of the CDM assume more complicated forms, namely quartic potentials.

The free parameters of the model have been chosen by requiring that the calculated static properties of the nucleon agree best with the experimental values ². In the version of the CDM with a quadratic potential, the results are predominantly sensitive to the quantity $G = \sqrt{gM_\chi}$; we take $G = 0.2$ GeV (and $g = 0.03$ GeV). The model contains other parameters: the pion decay constant, $f_\pi = 0.093$ GeV, the pion mass, $m_\pi = 0.14$ GeV, and the sigma mass, which we take in the range $0.7 \leq m_\sigma \leq 1.2$ GeV.

The nucleon is constructed by placing three valence quarks in the lowest s-state, i.e., the quark source can be written as $(1s)^3$ ³. For the Roper the quark source is $(1s)^2(2s)^1$, i.e. one of the three quarks now occupies the first (radially) excited state. The quarks are surrounded by a cloud of pions, sigma mesons and chi field, described by radial profiles $\phi(r)$, $\sigma(r)$ and $\chi(r)$ respectively. The hedgehog ansatz is assumed for the quarks and pions. The quark profiles (described in terms of the upper, u , and the lower component, v) and boson profiles are determined self-consistently.

Because of the hedgehog structure, the solution is neither an angular momentum eigenstate nor an isospin eigenstate, and therefore it cannot be related directly with a physical baryon. However, the physical states can be obtained from the hedgehog by first interpreting the solution as a coherent state of three types of bosons and then performing the Peierls-Yoccoz projection ^{1,13}:

$$|N_{\frac{1}{2}, M_T}\rangle = \mathcal{N} P_{\frac{1}{2}, -M_T}^{\frac{1}{2}} |Hh\rangle, \quad |R'_{\frac{1}{2}, M_T}\rangle = \mathcal{N}' P_{\frac{1}{2}, -M_T}^{\frac{1}{2}} |Hh^*\rangle, \quad (10)$$

where P is the projector and we introduced the symbol $*$ to denote the Roper intrinsic state. Because of their trivial tensor nature, the χ and the σ -fields are not affected by projection. This approach can be considerably improved by determining the radial profiles $\phi(r)$, $\sigma(r)$ and $\chi(r)$, as well as the quark profiles, using the variation after projection method ¹, separately for the nucleon and for the Roper.

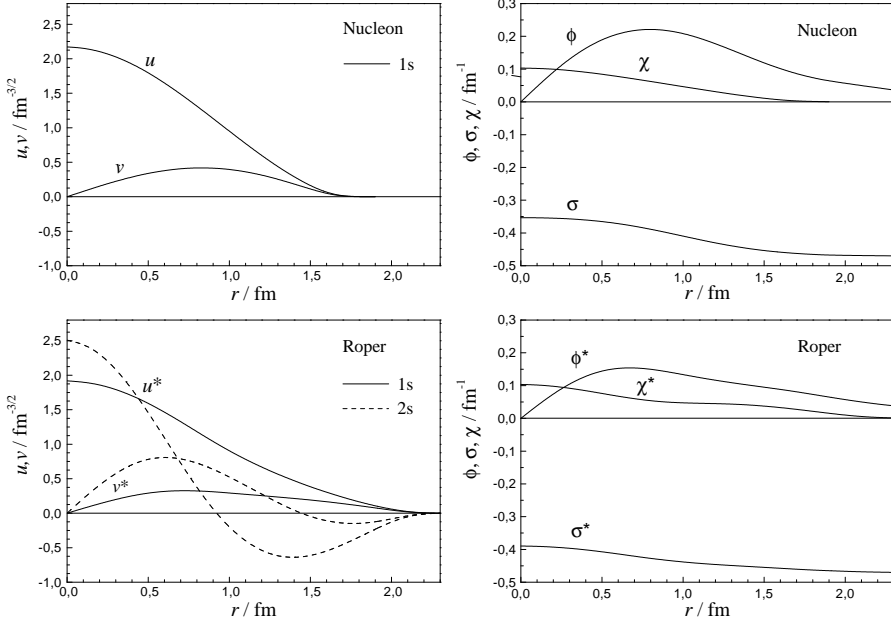


Figure 1. Quark and meson radial wave functions for the $(1s)^3$ (Nucleon) and $(1s)^2(2s)^1$ (Roper) configurations. The vacuum expectation value of the sigma field is $-f_\pi$. Note that the effective quark mass is proportional to the *inverse* of the χ field. We use the symbol $*$ to denote the Roper radial functions. The model parameters are: $M_\chi = 1.4$ GeV, $g = 0.03$ GeV, $m_\pi = 0.14$ GeV, $f_\pi = 0.093$ GeV, $m_\sigma = 0.85$ GeV.

Figure 1 shows the radial profiles for the $(1s)^3$ and $(1s)^2(2s)^1$ configurations. Those corresponding to the Roper extend further. The strength of the chiral mesons is reduced in the Roper in comparison with the nucleon. Another interesting feature is the waving shape acquired by the Roper chromodielectric field, χ^* . A central point in our treatment of the Roper is the freedom of the chromodielectric profile, as well as of the chiral meson profiles, to adapt to a $(1s)^2(2s)^1$ configuration. Therefore, quarks in the Roper experience meson fields which are different from the meson fields felt by the quarks in the nucleon. As a consequence, states (10) are normalized but not mutually orthogonal. They can be orthogonalized taking

$$|R\rangle = \frac{1}{\sqrt{1-c^2}}(|R'\rangle - c|N\rangle), \quad c = \langle N|R'\rangle. \quad (11)$$

A better procedure results from a diagonalization of the Hamiltonian in the

subspace spanned by (non-orthogonal) $|R'\rangle$ and $|N\rangle$:

$$|\tilde{R}\rangle = c_R^R|R'\rangle + c_N^R|N\rangle, \quad |\tilde{N}\rangle = c_R^N|R'\rangle + c_N^N|N\rangle. \quad (12)$$

In Table 1 the nucleon energies and the nucleon-Roper mass splitting are given. The absolute value of the nucleon energy is above the experimental value but it is known² that the removal of the center-of-mass motion will lower those values by some 300 MeV (similar correction applies to the Roper). On the other hand, the nucleon-Roper splitting is small, even in the case of the improved state (12). The smallness of the splitting is probably related with a much too soft way of imposing confinement.

Table 1. Nucleon energies and nucleon-Roper splittings for two sigma masses. E_N is the energy of the nucleon state (10), ΔE was obtained using (11), \tilde{E} and $\Delta \tilde{E}$ are calculated using the states (12). The other model parameters are in the caption of Figure 1. All values are in MeV.

m_σ	E_N	ΔE	\tilde{E}_N	$\Delta \tilde{E}$
700	1249	367	1235	396
1200	1269	354	1256	380

4 Amplitudes

Our results for the transverse helicity amplitudes are shown in Figure 2 for the parameter set used for Figure 1. The experimental values at the photon point

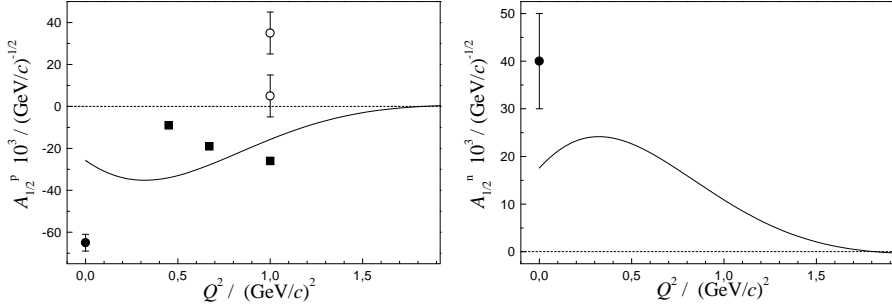


Figure 2. Nucleon-Roper transverse amplitudes. The experimental points at $Q^2 = 0$ GeV 2 are the estimates of the PDG¹⁴. The solid squares¹⁵ and the open circles¹⁶ result from the analysis of electroproduction data.

are the PDG most recent estimate ¹⁴ $A_{1/2}^p = -0.065 \pm 0.004$ $(\text{GeV}/c)^{-1/2}$ and $A_{1/2}^n = 0.040 \pm 0.010$ $(\text{GeV}/c)^{-1/2}$. The pion contribution to the charged states only accounts for a few percent of the total amplitude. The discrepancies at the photon point can be attributed to a too weak pion field, which we already noticed in the calculation of nucleon magnetic moments ² and of the electroproduction of the Δ ³. Other chiral models ¹² predict a stronger pion contribution which enhances the value of the amplitudes. If we calculate perturbatively the leading pion contribution we also find a strong enhancement at the photon point; however, when we properly orthogonalize the state with respect to the nucleon, this contribution almost disappears.

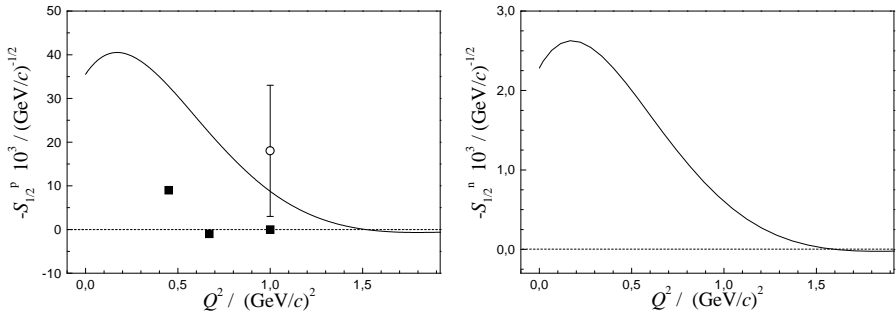


Figure 3. Nucleon–Roper scalar helicity amplitudes (see also caption of Figure 2).

In Figure 3 we present the scalar amplitudes. For the neutron no data are available which prevents any judgment of the quality of our results.

In CQM calculations ^{4,5,6} which incorporate a consistent relativistic treatment of quark dynamics, the amplitudes change the sign around $Q^2 \sim 0.2$ – 0.5 $(\text{GeV}/c)^2$. The amplitudes with this opposite sign remain large at relatively high Q^2 , though, as shown in ^{5,6}, the behavior at high Q^2 can be substantially reduced if either corrections beyond the simple Gaussian-like ansatz or pionic degrees of freedom are included in the model. Other models, in particular those including exotic (gluon) states, do not predict this type of behavior ¹⁷. The present experimental situation is unclear. Our model, similarly as other chiral models ^{12,18}, predicts the correct sign at the photon point, while it does not predict the change of the sign at low Q^2 . Let us also note that with the inclusion of a phenomenological three-quark interaction Cano *et al.* ⁶ shift the change of the sign to $Q \sim 1$ $(\text{GeV}/c)^2$ beyond which, in our opinion, predictions of low energy models become questionable anyway.

5 Meson excitations

The ansatz (10) for the Roper represents the breathing mode of the three valence quarks with the fields adapting to the change of the source. There is another possible type of excitation in which the quarks remain in the ground state while the χ -field and/or the σ -field oscillate. The eigenmodes of such vibrational states are determined by quantizing small oscillations of the scalar bosons around their expectation values in the ground state¹⁹. We have found that the effective potential for such modes is *repulsive* for the χ -field and *attractive* for the σ -field. This means that there are no glueball excitations in which the quarks would act as spectators: the χ -field oscillates only together with the quark field. On the other hand, the effective σ -meson potential supports at least one bound state with the energy ε_1 of typically 100 MeV below the σ -meson mass.

We can now extend the ansatz (11) by introducing

$$|R^*\rangle = c_1|R\rangle + c_2\tilde{a}_\sigma^\dagger|N\rangle, \quad (13)$$

where \tilde{a}_σ^\dagger is the creation operator for this lowest vibrational mode. The coefficients c_i and the energy are determined by solving the (generalized) eigenvalue problems in the 2×2 subspace. The lowest energy solution is the Roper while its orthogonal combination could be attributed to the $N(1710)$, provided the σ -meson mass is sufficiently small. In such a case the latter state is described as predominantly the σ -meson vibrational mode rather than the second radial excitation of quarks. This would manifest in very small production amplitudes since mostly the scalar fields are excited.

The presence of σ -meson vibrations is consistent with the recent phase shift analysis by Krehl *et al.*²⁰ who found that the resonant behavior in the P_{11} channel can be explained solely through the coupling to the σ -N channel. In our view, radial excitations of quarks are needed in order to explain relatively large electroproduction amplitudes, which would indicate that the σ -N channel couples to all nucleon $\frac{1}{2}^+$ excitations rather than be concentrated in the Roper resonance alone.

This work was supported by FCT (POCTI/FEDER), Portugal, and by The Ministry of Science and Education of Slovenia. MF acknowledges a grant from GTAE (Lisbon), which made possible his participation in EM12001.

References

1. M. C. Birse, *Prog. Part. Nucl. Phys.* **25**, 1 (1990); T. Neuber, M. Fiolhais, K. Goeke and J. N. Urbano, *Nucl. Phys. A* **560**, 909 (1993)

2. A. Drago, M. Fiolhais and U. Tambini, *Nucl. Phys. A* **609**, 488 (1996)
3. M. Fiolhais, B. Golli and S. Širca, *Phys. Lett. B* **373**, 229 (1996); L. Amoreira, P. Alberto and M. Fiolhais, *Phys. Rev. C* **62**, 045202 (2000);
4. S. Capstick, *Phys. Rev. D* **46**, 2864 (1992); S. Capstick and B.D. Keister, *Phys. Rev. D* **51**, 3598 (1995)
5. F. Cardarelli, E. Pace, G. Salmè and S. Simula, *Phys. Lett. B* **397**, 13 (1997)
6. F. Cano and P. González, *Phys. Lett. B* **431**, 270 (1998)
7. W. Broniowski, T. D. Cohen and M. K. Banerjee, *Phys. Lett. B* **187**, 229 (1987)
8. P. A. M. Guichon, *Phys. Lett. B* **163**, 221 (1985); *Phys. Lett. B* **164**, 361 (1985)
9. P. Alberto, M. Fiolhais, B. Golli and J. Marques, hep-ph/0103171, *Phys. Lett. B* **523**, 273 (2001)
10. R. Alkofer, H. Reinhardt and H. Weigel, *Phys. Rep.* **265** (1996) 139; C. V. Christov, A. Blotz, H.-C. Kim, P. V. Pobylitsa, T. Watabe, Th. Meissner, E. Ruiz Arriola and K. Goeke, *Prog. Part. Nucl. Phys.* **37** (1996) 1; B. Golli, W. Broniowski and G. Ripka, *Phys. Lett. B* **437** (1998) 24; B. Golli, W. Broniowski and G. Ripka, hep-ph/0107139
11. A. Silva, D. Urbano, T. Watabe, M. Fiolhais and K. Goeke, *Nucl. Phys. A* **675**, 637 (2000) ; D. Urbano, A. Silva, M. Fiolhais, T. Watabe and K. Goeke, *Prog. Part. Nucl. Phys.* **44**, 211 (2000)
12. K. Bermuth, D. Drechsel and L. Tiator, *Phys. Rev. D* **37**, 89 (1988)
13. B. Golli and M. Rosina, *Phys. Lett. B* **165**, 347 (1985); M. C. Birse, *Phys. Rev. D* **33**, 1934 (1986)
14. D. E. Groom et al. (Particle Data Group), *Eur. Phys. J. C* **15**, 1 (2000)
15. C. Gerhardt, *Z. Phys. C* **4**, 311 (1980)
16. B. Boden and G. Krosen, in Proc. of the Conference on Research Program at CEBAF II, eds. V. Burkert et al., CEBAF (USA), 1986
17. Zhenping Li, V. Burkert and Zhujun Li, *Phys. Rev. D* **46**, 70 (1992); E. Carlson and N. C. Mukhopadhyay, *Phys. Rev. Lett.* **67** 3745 (1991)
18. Y. B. Dong, K. Shimizu, A. Faessler and A. J. Buchmann, *Phys. Rev. C* **60**, 035203 (1999)
19. B. Golli, P. Alberto and M. Fiolhais, talk presented at the Mini-Workshop on *Few body problems in hadronic and atomic physics*, Bled, Slovenia, 7-14 July 2001, hep-ph/0111399
20. O. Krehl, C. Hanhart, S. Krewald and J. Speth, *Phys. Rev. C* **62**, 025207 (2000)